A&A 579, A58 (2015)
DOI: 10.1051/0004-6361/201425551

Astronomy & Astrophysics

A search for lithium in metal-poor L dwarfs⋆,⋆⋆,⋆⋆⋆

N. Lodieu[1,2], A. J. Burgasser[1,2,3,‡], Y. Pavlenko[4,5], and R. Rebolo[1,2,6]

[1] Instituto de Astrofísica de Canarias (IAC), Calle vía Láctea s/n, 38200 La Laguna, Tenerife, Spain
e-mail: [nlodieu;rrl]@iac.es
[2] Departamento de Astrofísica, Universidad de La Laguna (ULL), 38206 La Laguna, Tenerife, Spain
[3] Center for Astrophysics and Space Science, University of California San Diego, La Jolla, CA 92093, USA
[4] Main Astronomical Observatory of the National Academy of Sciences of Ukraine, 03680 Kyiv, Ukraine
[5] Center for Astrophysics Research, University of Hertfordshire, College Lane, Hatfield, Hertfordshire AL10 9AB, UK
[6] Consejo Superior de Investigaciones Científicas, CSIC, Spain

Received 19 December 2014 / Accepted 25 May 2015

ABSTRACT

Aims. The aim of the project is to search for lithium in absorption at 6707.8 Å to constrain the nature and mass of the brightest low-metallicity L-type dwarfs (referred to as L subdwarfs) identified in large-scale surveys.
Methods. We obtained low- to intermediate-resolution (R ~ 2500–9000) optical (~560–770 nm) spectra of two mid-L subdwarfs, SDSS J125637.13−022452.4 (SDSS1256; sdL3.5) and 2MASS J162620.14+392519.5 (2MASS1626; sdL4) with spectrographs on the European Southern Observatory Very Large Telescope and the Gran Telescopio de Canarias.
Results. We report the presence of a feature at the nominal position of the lithium absorption doublet at 6707.8 Å in the spectrum of SDSS1256, with an equivalent width of 66 ± 27 Å at 2.4σ, which we identify as arising from a CaH molecular transition based on atmosphere models. We do not see any feature at the position of the lithium feature in the spectrum of 2MASS1626. The existence of overlapping molecular absorption sets a confusion detection limit of [Li/H] = −3 for equivalently typed L subdwarfs. We provided improved radial velocity measurements of −126±10 km s^{-1} and −239±12 km s^{-1} for SDSS1256 and 2MASS1626, respectively, as well as revised Galactic orbits. We implemented adjusting factors for the CaH molecule in combination with the NextGen atmosphere models to fit the optical spectrum of SDSS1256 in the 6200–7300 Å range. We also estimate the expected Li abundance from interstellar accretion ([Li/H] = −5), place limits on circumstellar accretion (10^9 g/yr), and discuss the prospects of Li searches in cooler L and T subdwarfs.

Key words. techniques: spectroscopic – brown dwarfs – subdwarfs

1. Introduction

Stars spend most of their lifetimes on the main sequence in hydrostatic equilibrium and burning hydrogen. On the contrary, brown dwarfs never reach core temperatures and pressures high enough to fuse hydrogen (Kumar 1963; Hayashi & Nakano 1963). Lithium (Li) is destroyed in stellar interiors via collisions with protons. At solar metallicities brown dwarfs with masses below 0.065 $M_\odot$ do not reach the temperatures needed for Li I burning (Magazzu et al. 1991; Rebolo et al. 1992; Basri et al. 1996). The precise mass below which Li I is preserved depends on metallicity and, according to models, it could be higher at lower metallicities (Burrows & Liebert 1993; Chabrier & Baraffe 1997; Bildsten et al. 1997; Baraffe et al. 1998; Chabrier & Baraffe 2000; Burke et al. 2004).

Low-resolution optical spectroscopy of solar-metallicity nearby L dwarfs suggests early-L dwarfs represent a mixture of low-mass stars and brown dwarfs, whereas most objects with spectral types later than ~L5 are substellar. From a large sample of nearby L dwarfs with optical spectra, Kirkpatrick et al. (2008) showed that 10–20% of L0–L2 dwarfs exhibit Li in absorption, the percentage increasing to 40–80% for mid- to late-L dwarfs. This trend is corroborated by other works, e.g. Tinney (1998), Kirkpatrick et al. (1999, 2000), Pavlenko et al. (2007a), Cruz et al. (2009), and Zapatero Osorio et al. (2014). In the T dwarf regime, only Luhman 16B is known to harbour Li in absorption with an equivalent width of ~8 Å (Faherty et al. 2014; Lodieu et al. 2015) whereas Li is undetected in Gl 229 B (Schultz et al. 1998; Oppenheimer et al. 1998) and in the two component of Epsilon Indi B (King et al. 2010). Lithium remains undetected in the optical spectrum of another 17 T dwarfs (Burgasser et al. 2003b; Kirkpatrick et al. 2008; Leggett et al. 2012).

Ultracool subdwarfs (or Population II ultracool dwarfs) are defined as metal-poor dwarfs with spectral types later than M7. They appear bluer than the main-sequence solar-metallicity stars due to the lack of metals in their atmospheres (Mould & Hyland 1976; Baraffe et al. 1997). They usually exhibit halo kinematics, including high proper motions and large heliocentric velocities (Gizis 1997). They are important tracers of the chemical enrichment history of the Galaxy because they belong to the first generations of stars. The current compendium of

‡ Visiting professor at the Instituto de Astrofísica de Canarias (IAC), La Laguna, Tenerife, Spain.
⋆ Optical spectra of SDSS1256 and 2MASS 1626 are only available at the CDS via anonymous ftp to cdsarc.u-strasbg.fr (130.79.128.5) or via http://cdsarc.u-strasbg.fr/viz-bin/qcat?J/A+A/579/A58
⋆⋆ Based on observations collected at the European Southern Observatory, Chile, under programmes 089.C-0883 and 091.C-0594A.
⋆⋆⋆ Based on observations made with the Gran Telescopio Canarias (GTC), installed in the Spanish Observatorio del Roque de los Muchachos of the Instituto de Astrofísica de Canarias, in the island of La Palma (programmes GTC64_10B and GTC38_11A).

Table 1. Properties of the two mid-L subdwarfs presented in this paper.

RA	Dec	SpT	SDSSr	$\mu_\alpha \cos\delta$	μ_δ	Dist	$EW_{\rm Li}$	RV	(U, V, W)
hh:mm:ss.ss	°:′:″		mag	mas/yr	mas/yr	pc	mÅ	km s^{-1}	(km s^{-1}, km s^{-1}, km s^{-1})
12:56:37.13	−02:24:52.4	sdL3.5	21.82	−741.1 ± 1.4	−1002.0 ± 1.4	53.3 ± 6.8	<66 ± 27	−126 ± 10	(−62 ± 6, −227 ± 37, −224 ± 18)
16:26:20.14	+39:25:19.5	sdL4.0	20.65	−1374.1 ± 1.0	+238.0 ± 0.9	33.5 ± 1.3	≤90	−239 ± 12	(−166 ± 6, −261 ± 9, −2 ± 11)

Notes. Listed are the names, coordinates, spectral types (Burgasser 2007; Burgasser et al. 2009), Sloan r-band magnitude (Adelman-McCarthy et al. 2007, 2009), proper motions, distances (Schilbach et al. 2009), final upper limits on the Li I pseudo-equivalent widths, radial velocities, and revised space motion (this paper).

Table 2. Li I EWs (3σ upper limits) from low-resolution spectra published in the literature, as measured here (see Sect. 4).

Source	SpType	EW(Li I)	Reference
		Å	
SDSS J1256−0122	sdL3.5	<1.1	B07
2MASS J1626+3925	sdL4.0	<0.4	B07
2MASS J0616−6407	sdL5.0	<2.0	C09
2MASS J0532+8246	sdL7.0	<0.6	B03
2MASS J0645−6646	sdL8.0	<3.6	K10

Notes. References are: B03 (Burgasser et al. 2003a); B07 (Burgasser et al. 2007); C09 (Cushing et al. 2009); and K10 (Kirkpatrick et al. 2010).

ultracool subdwarfs contains approximately 50 objects, in particular 11 L-type subdwarfs (Burgasser et al. 2003a; Burgasser 2004; Cushing et al. 2009; Sivarani et al. 2009; Lodieu et al. 2010, 2012; Kirkpatrick et al. 2010, 2014).

Because M subdwarfs are old components of our Galaxy (a few Gyr) with effective temperatures in the 3000–4000 K range (Rajpurohit et al. 2014) we do not expect to detect lithium in absorption in their optical spectra because all the Li has been burnt. However, L subdwarfs are very low-mass objects at low metallicities and are likely to have masses close to the minimum needed for Li I burning. Lithium is expected to be present in the formation of subdwarfs at high abundances given its origin in Big Bang nucleosynthesis (Spite & Spite 1982; Rebolo et al. 1988; Bonifacio et al. 2007). Hence, L subdwarfs might have preserved a significant amount of primordial Li I in their atmospheres if they are substellar. To enable the detection of the Li I resonance doublet at 6707.8 Å, it is advisable to focus on the coolest subdwarfs known, with effective temperatures below ~2000–2500 K. However, the faint continua of L subdwarfs around the Li I feature at 6707.8 Å necessitates observations of sufficient resolution and sensitivity to firmly establish its presence or absence. For depletion factors in the range 2–100, theoretical models predict equivalent widths (EW) between 0.3 Å and 0.8 Å (Pavlenko et al. 1995). Prior low-resolution optical observations did not have sufficient signal-to-noise ratio to do this (Table 2; Burgasser et al. 2003a; Cushing et al. 2009; Burgasser et al. 2009; Kirkpatrick et al. 2010).

In this paper we present medium-resolution optical spectra of two mid-L subdwarfs, SDSS J125637.13−022452.4 (hereafter SDSS1256; sdL3.5; Sivarani et al. 2009; Burgasser et al. 2009) and 2MASS J162620.14+392519.5 (hereafter 2MASS1626; sdL4; Burgasser et al. 2007), obtained with the European Southern Observatory (ESO) Very Large Telescope (VLT) in Paranal (Chile) and the Gran Telescopio de Canarias (GTC) in the Roque de Los Muchachos Observatory on La Palma (Canary Islands). We selected these two subdwarfs because they are the brightest in their class. Their properties are summarised in Table 1. In Sect. 2, we describe the spectroscopic observations conducted in service mode by ESO and GTC. In Sects. 3 and 6, we present refined radial velocities yielding improved 3D space motions as well as luminosities and effective temperatures for both objects. In Sect. 4, we discuss our analysis of the lithium absorption in the optical spectra of both mid-L subdwarfs. In Sect. 5, we compare our upper limits on the pseudo-equivalent widths of the Li I feature with theoretical predictions to place a limit on the mass of the subdwarfs. In Sect. 7 we place our results in context and discuss the opportunity offered to detect lithium in halo brown dwarfs.

2. Spectroscopic observations

2.1. GTC/OSIRIS optical spectroscopy

We obtained optical spectroscopy of 2MASS1626 with the OSIRIS (Optical System for Imaging and low-intermediate Resolution Integrated Spectroscopy; Cepa et al. 2000) spectrograph mounted on the 10.4 m GTC telescope in La Palma. Observations were conducted in February and April 2011 over two semesters under programmes GTC64_10B and GTC38_11A (PI Espinoza Contreras; Table 3).

OSIRIS is equipped with two 2048 × 4096 Marconi CCD42-82 detectors offering a field of view approximately 7 × 7 arcmin with an unbinned pixel scale of 0.125 arcsec. We employed the R2500R grating with a slit width of one arcsec giving a resolution of ~2400 under dark or grey conditions, variable seeing between 0.8 and 1.6 arcsec, and clear skies. We obtained three exposures shifted along the slit with on-source integrations of 1402 s on 5 February 2011, another three with the same on-source integrations on 12 February 2011, and two additional exposures of 1636 s on 13 April 2011. Bias frames, dome flat fields, and Ne, Xe, and HgAr arc lamps were observed by the observatory staff during the afternoon preceding or following the observations.

We carried out the data reduction of the optical spectra under the IRAF environment (Tody 1986, 1993)[1]. We subtracted the raw median-combined bias frame from the raw spectrum and divided by a normalised dome flat field. We extracted each spectrum individually without combining them to avoid shifts due to the large space velocity of the target and the position of the Earth at the time of the observations. We chose an optimal sky background and aperture to extract the one-dimensional (1D) spectrum. We calibrated our spectrum in wavelength with arc lamps

[1] IRAF is distributed by the National Optical Astronomy Observatories, which are operated by the Association of Universities for Research in Astronomy, Inc., under cooperative agreement with the National Science Foundation.

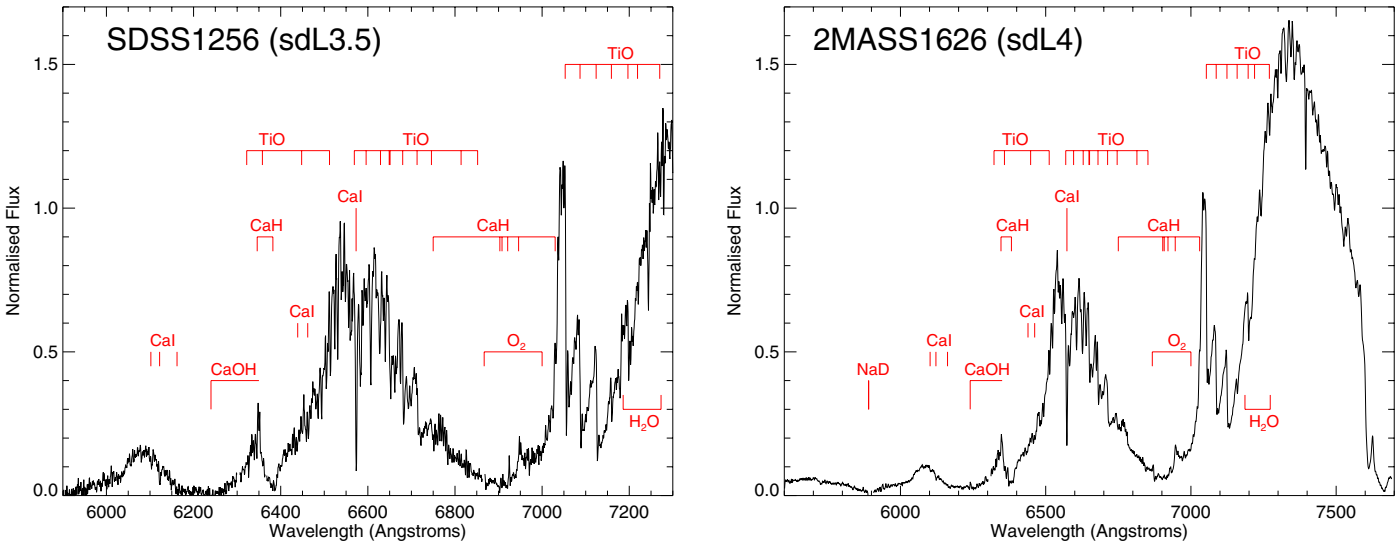

Fig. 1. Full combined optical spectra of SDSS1256 (*left*) and 2MASS1626 (*right*) obtained with VLT/FORS2 and GTC/OSIRIS, respectively. Both spectra are in the Earth frame and have been arbitrarily normalised at 7050 Å. Some important bands and features seen in metal-poor dwarfs are marked in red.

Table 3. Log of the spectroscopic observations for SDSS1256 and 2MASS1626 with VLT/FORS2 (1200R+93) and GTC/OSIRIS (R2500), respectively.

Name	Tel. Inst.	Date	ExpTime
		dd/mm/yy	s
SDSS1256	ESO VLT FORS2	27/04/12	2824
		21/06/12	2824
		03/04/13	2824[a]
		11/04/13	2 × 2824
		12/04/13	2824
		14/04/13	2 × 2824
2MASS1626	GTC OSIRIS	05/02/11	3 × 1682
		12/02/11	3 × 1682
		13/04/11	2 × 1682

Notes. We give the dates of observations and the integration times with the number of individual exposures (in case of multiple ones) for each spectrum obtained for each target. [(a)] This spectrum is not used in our analysis owing to the presence of a strong cosmic ray at the position of the Li I.

with an accuracy better than 0.05 Å rms. Finally, we calibrated each 1D spectrum in flux with the spectro-photometric standard stars G191-B2B (DA.8; van Leeuwen 2007; Høg et al. 2000; Gianninas et al. 2011) and Ross 640 (DZ5; Harrington & Dahn 1980; Sion et al. 2009; Lépine & Shara 2005). The individual spectra were shifted by the barycentric velocities corresponding to the times of observations, then combined with uncertainty weighting. The final combined optical spectrum of 2MASS1626 is displayed in the right panel in Fig. 1. The signal-to-noise ratio around the Li doublet is 90–100.

2.2. VLT/FORS2 optical spectroscopy

We obtained intermediate-resolution ($R \sim 9000$) optical spectroscopy of SDSS1256 with the visual and near UV FOcal Reducer and low dispersion Spectrograph (FORS2; Appenzeller et al. 1998) mounted on the ESO 8.2 m VLT at the Cerro Paranal observatory in Chile. We collected eight optical spectra over two semesters under programmes 089.C-0883A and 091.C-0594A (PI Espinoza Contreras; Table 3) under grey time, clear skies, and a seeing better than one arcsec.

FORS2 is a multi-mode instrument mounted on the UT1 Cassegrain focus working at optical wavelengths. We used the standard resolution collimator providing a pixel scale of 0.25 arcsec and a field of view of 6.8 arcmin by 6.8 arcmin. We employed the grism GRIS_1200R+93 associated with its order separation filter GG435 with a slit width of one arcsec to achieve a spectral resolving power of ~9000 around the Li I doublet. We obtained eight exposures of 2824 s in April and June 2012 and April 2013 (Table 3), yielding a total on-source integration of ~6.3 h and a signal-to-noise ratio of 50–60 around 6700 Å. However, we do not use the spectrum taken on 03 April 2013 because the Li I region is affected by a strong cosmic ray. Bias frames, dome flat fields, and arc lamps were taken by the observatory staff during the afternoon.

We performed the data reduction of the FORS2 datasets in a similar way as the OSIRIS under IRAF. We subtracted the raw median-combined bias frame from each raw spectrum, divided each of them by a normalised dome flat field, and extracted a 1D spectrum calibrated in wavelength to an accuracy better than 0.05 Å rms. Finally, we calibrated each spectrum in flux with the spectro-photometric standard stars LTT 6248 (A; Høg et al. 2000; Pancino et al. 2012) and LTT 7379 (G0; van Altena et al. 1995; Gontcharov 2006; van Leeuwen 2007; Pancino et al. 2012). The final combined optical spectrum of SDSS1256 is shown in the left panel in Fig. 1.

3. Improved radial velocities and space motions

We took advantage of the medium-resolution data for SDSS1256 and 2MASS1626 to improve their radial velocities. We first measured the offsets of the strong CaI line at 6572.78 Å[2], averaging measurements from each individual spectrum. For SDSS1256 we obtained a mean offset of $1.5^{+0.4}_{-0.3}$ Å after rejecting the value obtained on 22 June 2012, which is discrepant

[2] Air wavelength from the NIST database http://physics.nist.gov/PhysRefData/ASD/lines_form.html

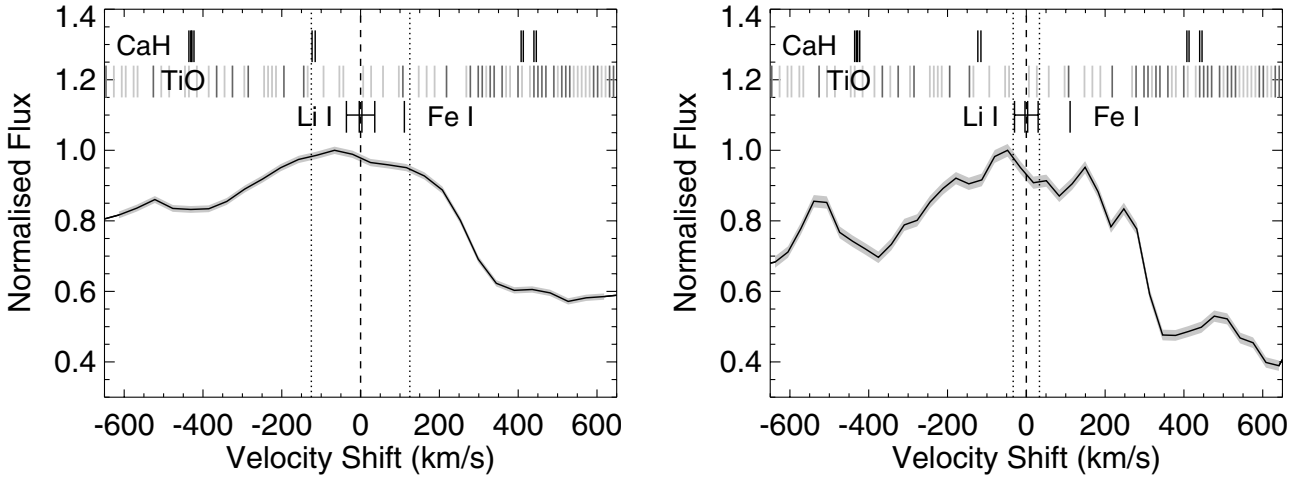

Fig. 2. Zoom-in on the combined spectra (black line) for SDSS1256 (*left*) and 2MASS1626 (*right*) around the Li I line. The grey bands indicate the formal spectral uncertainties while the horizontal error bar indicates the 3σ radial velocity uncertainties. Dotted lines indicate the velocity resolution of the instruments used. Overplotted at the *top* are marked the main features of CaH, Li, Fe, and TiO. We note that TiO is blanketing the entire region with cross-sections of various strengths from 5×10^{-17}, 1×10^{-16}, 5×10^{-16} cm^2/molecules shown in three shades of grey (light to dark).

by 3σ. Assuming a spectral resolution of 0.73 Å equivalent to 33 km s^{-1} for the FORS2 configuration used, we derive a mean radial velocity of -152^{+14}_{-24} km s^{-1}, consistent with the values of -98.4 km s^{-1}, -90 ± 40 km s^{-1}, and -130 ± 11 km s^{-1} derived by West et al. (2008), Sivarani et al. (2009), and Burgasser et al. (2009), respectively. For 2MASS1626 we derived a mean offset of $-4.60^{+0.43}_{-0.72}$ Å, which translates into a radial velocity shift of $-211.6^{+19.8}_{-33.1}$ km s^{-1} assuming a spectral resolution of 1.028 Å for the GTC/OSIRIS configuration. This estimate agrees within 1.5σ with the value of -260 ± 35 km s^{-1} reported by Burgasser (2004).

We have also measured the radial shifts by cross-correlating both spectra around the 7000–7150 Å TiO band to zero-velocity using SDSS templates from Bochanski et al. (2007). We used M7, M8, and M9 templates as these provided the closest matches to the enhanced TiO band present in these L subdwarfs (Burgasser et al. 2007, see Sect. 5). By correlating each of the individual spectra and averaging, we infer radial velocities of -122 ± 9 km s^{-1} for SDSS1256 and -243 ± 13 km s^{-1} for 2MASS1626, where the uncertainties account for scatter between observations and templates. These velocities are in agreement with our line measurements, but with considerably improved accuracy. We adopt as our final values the uncertainty-weighted mean of our line and cross-correlation measurements, which are -126 ± 10 km s^{-1} for SDSS1256 and -239 ± 12 km s^{-1} for 2MASS1626. We also verified that these velocities aligned the two spectra at their rest wavelengths (Fig. 2) by checking the positions of a few lines (e.g. CaH at around 6698, 6705, 6717, and 6718 Å, FeI at 6710 Å, and TiO at 6695, 6704.5, and 6710 Å) and observed structures like the big central hump and the little bumps at -530 km s^{-1} and $+450$ km s^{-1}.

Moreover, we measured the pseudo-equivalent width (pEW) of the CaI line at 6571.10 Å, inferring a mean value of $3.54^{+0.18}_{-0.29}$ Å for SDSS1256 and $3.52^{+0.25}_{-0.40}$ Å for 2MASS1626, in excellent agreement, which is expected owing to the similarity in spectral type between the two targets.

We calculated UVW velocities for both sources based on our revised velocities and reported proper motions and distances (Schilbach et al. 2009), assuming a local right-handed Cartesian coordinate system with U pointed radially outward from the Galactic centre, V in the direction of Galactic rotation, and W in the direction of the Galactic north pole. We assumed local standard of rest (LSR) velocities of (11, 12.24, 7.25) km s^{-1} from Schönrich et al. (2010). Our values are reported in Table 1. For both sources values differ from those reported in Burgasser et al. (2007, 2009) primarily owing to the inclusion of the Schilbach et al. (2009) astrometry. Both exhibit V velocities that are almost perfectly counter Galactic rotation at the solar radius, 218 ± 6 km s^{-1} (Bovy et al. 2012).

We calculated revised Galactic orbits for both sources using these velocities, following the methods outlined in Burgasser et al. (2009), which are shown in Fig. 3. SDSS1256, whose galactocentric azimuthal velocity is nearly zero, exhibits a remarkable polar orbit that takes it completely around the Galactic bulge. 2MASS1626, which has a slightly retrograde azimuthal motion and very low W velocity, remains confined to the Galactic plane, but has an eccentric orbit that takes it within the inner kpc of the Galaxy. Neither source goes beyond a radial distance of 12 kpc from the Galactic centre. These orbital properties are consistent with membership to the inner halo population, implying a metallicity around [M/H] = −1.5 dex (Carollo et al. 2007).

4. The Li resonance doublet in mid-L subdwarfs

Focusing on the Li I region, we find that the combined spectrum of SDSS1256 shows a distinct but weak feature near the rest wavelength of the 6707.83 Å Li I line, centred within the radial velocity uncertainty. Using a linear fit to the adjacent peaks to estimate the pseudo-continuum, we measure $EW = 66 \pm 27$ mÅ for this feature, the uncertainty determined from the spectral errors and radial velocity uncertainty through Monte Carlo simulation. This 2.4σ detection is comparable in strength to several other features near the Li I line, so to assess both reliability and contamination we compared this spectrum to synthetic models, as discussed in Sect. 5.

For 2MASS1626, no distinct features are present, largely owing to the much lower resolution of the data. To quantify our limits, we inserted a Li I absorption feature at progressively

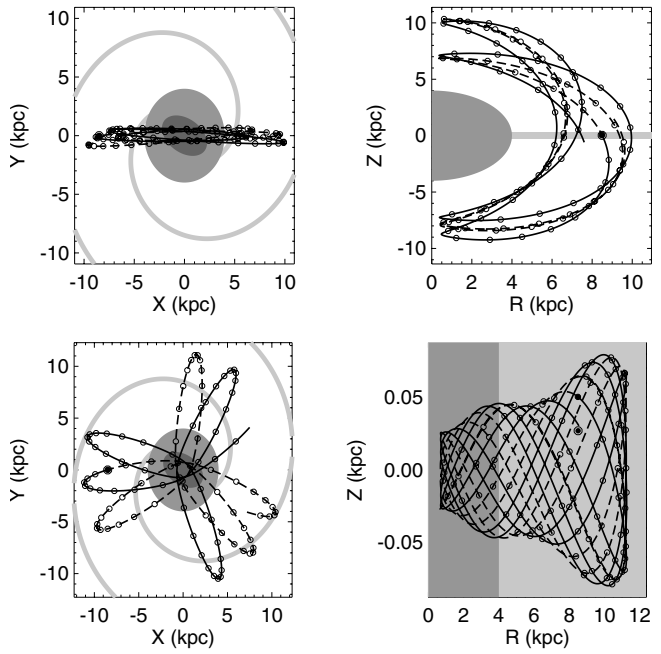

Fig. 3. Galactic orbits for SDSS1256 (*top*) and 2MASS1626 (*bottom*) over ~500 Myr as viewed from above the Galactic north pole (left) and in cylindrical coordinates (*right*). Future motion is indicated by solid lines, past motion by dashed lines, and points indicate 50 Myr steps. The Sun is located at $(X, Y) = (-8.5, 0)$ kpc. Representations of the Galactic bar (darkest grey), bulge (grey), and thin disk/major spiral arms (lightest grey) are also shown.

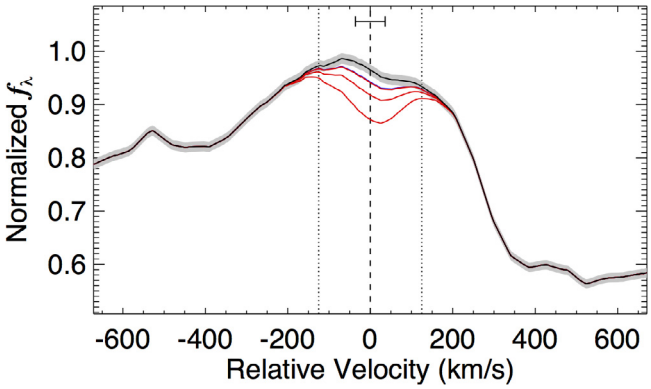

Fig. 4. Zoom-in on the spectral region containing the Li I feature (black), to which we added Gaussian line profile (red) with EWs of 100, 200, and 400 mÅ.

stronger EWs using a Gaussian line profile modelled from the 6572.78 Å CaI line. Figure 4 demonstrates that statistically significant deviations from the original spectrum occur for EW = 90 mÅ, but a clear feature can only be seen for an EW > 200 mÅ. We are clearly limited by systematics associated with the low resolution of these data and the underlying structure of the pseudocontinuum. The inferred limit is consistent with the best limits from prior low-resolution observations of L subdwarfs (Table 2), and well above the strength of the feature we infer for SDSS1256.

5. Comparison with theoretical models

To validate the possible presence of Li I in the spectrum of SDSS1256 and infer its atmospheric composition, we generated grids of synthetic spectra following the procedure outlined in Pavlenko et al. (2007a). We started with the NextGen model atmospheres of Allard et al. (2001) at solar metallicity. The profiles of the NaI and KI resonance doublets were computed in the framework of a quasi-static approach described in Pavlenko et al. (2007b) with an upgraded approach from Burrows et al. (2003). The line lists of VO and CaH were taken from Kurucz's website[3] with more details presented in Pavlenko (2014). The CrH and FeH line lists were computed by Burrows et al. (2002) and Dulick et al. (2003), respectively. We upgraded the TiO line lists of Plez (1998) with the new version available on his website[4]. The spectroscopic data for atomic absorption come from the Vienna Atomic Line Database (VALD; Kupka et al. 1999)[5].

[3] kurucz.harvard.edu

[4] http://www.pages-perso-bertrand-plez.univ-montp2.fr/

[5] http://vald.astro.univie.ac.at/~vald/php/vald.php

More details on the technique and procedure are presented in Pavlenko et al. (2006) in the case of the M6 dwarf GJ 406. Following Pavlenko (1998), we computed partial pressures of some molecules and atoms which exceeded the pressures of the gas-dust phase transition and decreased their gas phase abundances to the corresponding equilibrium values.

The best fit to the observed low-resolution spectrum of SDSS1256 (Burgasser et al. 2009) was obtained for an effective temperature of 2600 K and a log(g) surface gravity of 5.0 (cgs). To get a better fit we reduced the absorption of CrH theoretical bands by factor of two. This might be caused by a deficit of Cr atoms in the atmosphere or some depletion of Cr into dust particles. Then, we increased the absorption of CaH bands by factor of two, likely related to the well-known enhancement of calcium and other alpha-elements in the atmospheres of metal-poor dwarfs (Magain 1987). Moreover, we added some phenomenological dust opacity in the modelling of theoretical spectra, following the scheme of Pavlenko et al. (2007a). The wavelength-independent dust opacity of a total optical depth of $\tau = 0.3$ is located in a cloud-like layer at $\tau_{\rm ross} = 0.001$, i.e above the photosphere of the dwarf. These phenomenologically implemented parameters provide a much improved fit to the spectrum of SDSS1256, reproducing the strong CaH and TiO absorption bands between 6300 and 7200 Å, as well as individual metal lines in this region (right panel in Fig. 5). The most notable discrepancy between the synthetic spectra and the observed spectrum below 6300 Å is likely caused by incompleteness of the CaH linelist at these wavelengths. The full spectral energy distribution of the SDSS1256 from the optical up to the mid-infrared is also nicely reproduced by our synthetic spectra (Fig. 6). These adjusting parameters should be considered in the framework of more accurate investigation of abundances and chemical equilibrium in the atmospheres of metal-deficient L dwarfs because our parameters are actually not self-consistent with the temperature/pressure profile that generated the synthetic spectrum.

To assess the reality of the Li I absorption feature in the spectrum of SDSS1256, we examined the region around the Li I absorption doublet by fixing the adjusting factor for CaH to the aforementioned values and setting [Li/H] = −1, −2, −3, and −4 dex (corresponding to abundances of Li of 10, 100, 1000, and 10 000 less than solar, respectively). We note that the Li/H = −3.0 and −4.0 models are nearly identical because Li opacity has fallen below some other opacity source (mainly CaH). Our observed absorption is weaker than the two most depleted abundances, suggesting that our tentative detection is

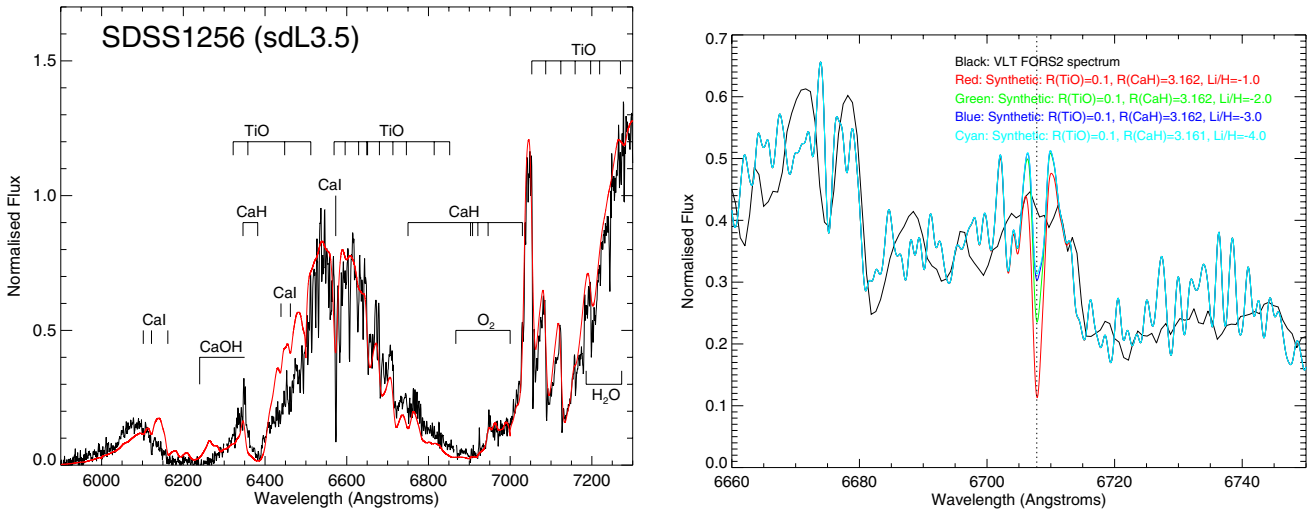

Fig. 5. *Left*: VLT/FORS2 observed spectrum of SDSS1256 (black line). Overplotted in red is the synthetic spectrum from the NextGen atmosphere models of Baraffe et al. (1998) generated with the DUST546 code of Pavlenko et al. (2007a), which provides the best fit to the data (a low-resolution version is shown for plotting purposes). The synthetic spectra, convolved by the instrument profile, have been generated for a metallicity of [M/H] = −2.0, gravity of $\log g = 5.0$, Li abundance of $\log N(\mathrm{Li}) = -1.0$. Both spectra are normalised to the observed spectrum around 7050 Å. Major lines and features present in optical spectra of metal-poor dwarfs are shown as well. *Right:* zoom-in on the region around the lithium doublet at 6707.8 Å. The observed spectrum is shown in black while synthetic spectra with different Li abundances are shown in colour.

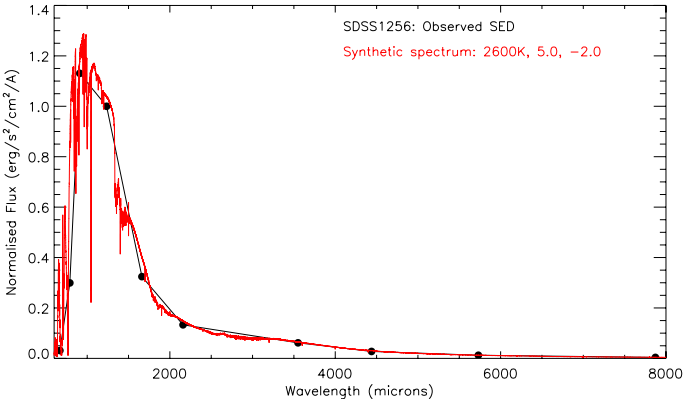

Fig. 6. Full spectral energy distribution of SDSS1256 from the optical all the way to the mid-infrared. Overplotted in red is the synthetic spectra from the atmosphere models of Allard et al. (2001) generated with the DUST546 code of Pavlenko et al. (2007a), which produces a satisfactory fit.

unlikely associated with Li and instead comes from a band most likely created by CaH or TiO. We can set an upper limit on the Li abundance in SDSS1256 to [Li/H] = −3.0. We conclude that low Li abundances in subdwarfs will remain a challenge to detect (see also Sect. 7.1).

6. Luminosities and effective temperatures

We determined the luminosities and effective temperatures of both subdwarfs following the procedure described in Burgasser et al. (2008). Previously published low-resolution optical and near-infrared spectral data (Burgasser 2004; Burgasser et al. 2007, 2009) spanning 0.6–2.5 microns were combined and scaled to 2MASS and SDSS photometry. These were joined to segments of a $T_{\rm eff} = 2000$ K, $\log g = 5.0$, solar-metallicity BT-Settl08 model (Allard et al. 2012) scaled to match SDSS and WISE photometry and *Spitzer*/IRAC measurements for 2MASS1626[6]. The combined spectrum was then scaled to absolute fluxes using the parallax measurements of Schilbach et al. (2009), and integrated over 0.3–30 microns (accounting for 99.96% of the total spectral model flux) to calculate bolometric fluxes and luminosities. We obtained radius estimates from the evolutionary models of Burrows et al. (2001), Baraffe et al. (2003), and Saumon & Marley (2008), assuming ages of 5–10 Gyr and the measured luminosities. Values are listed in Table 4, with uncertainties that include spectral, photometric and astrometric errors, and scatter in model radii. We also experimented with different spectral model sets, model $T_{\rm eff}$s spanning 1700–2400 K, and subsolar metallicity models ([M/H] = −1, −2); however, because the spectral model segments encompassed a small portion of the spectrum these variations were much smaller than the observational uncertainties. Varying the model parameters (i.e. the temperature by ±500 K and the gravity by ±0.5 dex) did not change the resulting effective temperature by more than 15 K.

Table 4. Bolometric luminosities ($\log_{10}(L_{\rm bol}/L_\odot)$), effective temperatures ($T_{\rm eff}$), and radii (R) for SDSS1256 and 2MASS1626.

Name	$\log_{10}(L_{\rm bol}/L_\odot)$	$T_{\rm eff}$	R
	dex	K	$R_\odot$
SDSS1256 (sdL3.5)	−3.93 ± 0.08	2000 ± 100	0.090 ± 0.003
2MASS1626 (sdL4.0)	−3.73 ± 0.02	2180 ± 30	0.095 ± 0.002

Our analysis reveals that SDSS1256 is 0.2 dex less luminous and nearly 200 K cooler than 2MASS1626, despite being classified 0.5 subtype earlier. This is confirmed by its fainter absolute infrared magnitudes ($M_{W1} = 11.49 \pm 0.30$ mag vs. $M_{W2} = 10.46 \pm 0.09$ mag). The seeming reversal in temperature trend with spectral type may reflect differing metallicities between these objects or possibly unresolved multiplicity (Goldman et al. 2008).

[6] Measured values are [3.6] = 13.27 ± 0.04 mag, [4.5] = 13.19 ± 0.04 mag, [5.8] = 13.03 ± 0.06 mag, and [8.0] = 12.95 ± 0.04 mag (DDT-225, PI Burgasser).

7. Discussion of the presence of lithium in halo brown dwarfs

7.1. Weak Li I in L subdwarfs from accretion

Given the absence of Li I absorption in excess of the overlapping molecular absorption feature, we infer that both L subdwarfs have depleted their lithium through core fusion and have masses above 0.065 $M_{\odot}$. Indeed, evolutionary models of Baraffe et al. (1997) show that metal-poor dwarfs with effective temperatures of 1900–2400 K have masses around 0.08 $M_{\odot}$ (Table 4) and have already depleted their lithium and lie on the main sequence; the stellar/substellar boundary is around 0.06 $M_{\odot}$ (with a spread of about 10%) at metallicities between −2.0 and −1.0 dex.

However, it would be conceivable that a low abundance of Li could be maintained in the photosphere from either the intersellar medium (ISM) or circumstellar material. We can estimate the observable abundance in either case assuming a steady-state photospheric composition, with accretion providing a Li source and convection and core fusion providing a Li sink:

$$\frac{\mathrm{d}(f_{\mathrm{Li,ph}} M_{\mathrm{ph}})}{\mathrm{d}t} \approx M_{\mathrm{ph}} \frac{\mathrm{d}f_{\mathrm{Li,ph}}}{\mathrm{d}t} \approx f_{\mathrm{Li,acc}} \frac{\mathrm{d}M_{\mathrm{acc}}}{\mathrm{d}t} - f_{\mathrm{Li,ph}} \frac{M_{\mathrm{ph}}}{t_{\mathrm{dep}}} = 0. \quad (1)$$

Here, $f_{\mathrm{Li,ph}}$ is the steady state mass fraction of Li in the photosphere; $f_{\mathrm{Li,acc}}$ the mass fraction of Li in the accreted material; M_{ph} is the constant mass of the photosphere, estimated as $10^{-10} M_{\mathrm{tot}} \approx 10^{-11} M_{\odot}$ (Burrows & Liebert 1993); $\mathrm{d}M_{\mathrm{acc}}/\mathrm{d}t$ is the instantaneous mass accretion rate in $M_{\odot}$/yr; and t_{dep} is the depletion time scale for Li by downward convection and core burning, assumed here to be 10 Myr. These assumptions yield

$$\frac{f_{\mathrm{Li,ph}}}{f_{\mathrm{Li,acc}}} \approx \frac{N_{\mathrm{Li,ph}}}{N_{\mathrm{Li,acc}}} \approx \frac{t_{\mathrm{dep}}}{M_{\mathrm{ph}}} \frac{\mathrm{d}M_{\mathrm{acc}}}{\mathrm{d}t} \approx 10^{19} \frac{\mathrm{d}M_{\mathrm{acc}}}{\mathrm{d}t} \mathrm{yr}/M_{\odot}. \quad (2)$$

The ISM accretion rate can be estimated from simple ballistic accretion[7]; i.e., a projectile of cross section πR^2 plunging through the ISM at a relative speed $v \approx 300$ km s^{-1} [8]. In this case,

$$\frac{\mathrm{d}M_{\mathrm{ISM}}}{\mathrm{d}t} \approx n_{\mathrm{H}} m_{\mathrm{H}} \pi R^2 v \approx N_{\mathrm{H}} m_{\mathrm{H}} \pi R^2 / t_{\mathrm{pass}} \approx 10^{-24}\ M_{\odot}/\mathrm{yr} \quad (3)$$

where the first expression is the instantaneous accretion rate and the second is averaged over the disk passage, assuming $n_{\mathrm{H}} = 1$ cm^{-3} and $N_{\mathrm{H}} = 10^{21}$ cm^{-2} (Kalberla & Kerp 2009), $R \approx R_{\mathrm{Jup}} = 7 \times 10^9$ cm, and a disk passage time of 1 Myr ($W = 200$ pc/Myr). For this rate:

$$\frac{N_{\mathrm{Li,ph}}}{N_{\mathrm{Li,ISM}}} \approx 10^{-5}. \quad (4)$$

For an Li ISM abundance consistent with primordial Big Bang nucleosysthesis ($\log N(\mathrm{Li}) = +2.6$ or [Li/H] = 1.5; Spergel et al. 2007; Lodders 2003) or hot halo stars ($\log N(\mathrm{Li}) = +2.0$ or [Li/H] = 0.9; Spite & Spite 1982; Fields 2011) this fraction corresponds to a photometric abundance of [Li/H] from −4 to −3, at or below our inferred confusion limit with CaH. Hence, it is unlikely that Li accreted from the ISM will be in sufficient abundance to be deteced in Li-burning L subdwarfs.

In the case of circumstellar accretion, solar meteoritic material has a Li abundance 20 times higher than hot halo stars ($\log N(\mathrm{Li})_{\mathrm{ISM}} = +2.2$; Lodders 2003), so the corresponding mass accretion rate can be 20 times lower to achieve the same basal abundance. For a detection threshold of [Li/H] = −3, we can rule out circumstellar accretion onto SDSS1256 at a rate higher than $\mathrm{d}M_{\mathrm{csm}}/\mathrm{d}t \approx 6 \times 10^{-25}\ M_{\odot}/\mathrm{yr} \approx 10^9$ g/yr, roughly equivalent to the meteoric accretion rate of Earth. While not enough is known about the formation of solid bodies around these low mass, metal-poor stars to make a quantitative assessment, this limit suggests that very little circumstellar material remains around these sources. We note that accretion of a larger planet could temporarily boost the lithium abundance, a mechanism that has been proposed for Li-rich red giants (Alexander 1967; Israelian et al. 2001; Carlberg et al. 2010); however, such an event must have happened quite recently (<10 Myr) for an excess to be observed before the accreted Li is convected to the core and destroyed.

7.2. Searches for lithium in cooler subdwarfs

Given the lack of Li in mid-type L subdwarfs, will we be able we confirm the substellar nature of halo brown dwarfs with the lithium test (Magazzu et al. 1991, 1992; Rebolo et al. 1992; Basri et al. 1996) in the near future? For solar-metallicity stellar and substellar chemistry (e.g. Burrows & Sharp 1999; Lodders & Fegley 2006), Li is predicted to be in atomic form above ∼1500–1700 K at 1 bar pressure but converted into molecules at lower temperatures. Hence, we would expect chemical depletion of Li for ultracool dwarfs below 1500 K, which seems supported by observations of the coolest L and T dwarfs (Kirkpatrick et al. 2008; King et al. 2010; Faherty et al. 2014; Lodieu et al. 2015).

Theoretical models locate the hydrogen-burning limit at higher masses (∼0.09 $M_{\odot}$ for $Z = 0$ vs. 0.075 $M_{\odot}$ for solar metallicity) and warmer temperatures for subsolar metallicities (Burrows et al. 1997; Chabrier & Baraffe 1997). From our results for the two mid-L subdwarfs presented in this paper, we can conclude that the Li burning limit lies below 2000 K, equivalent to masses below ∼0.08 $M_{\odot}$. The low-metallicity models of Baraffe et al. (1997) predict a Li boundary minimum masses around 0.06 $M_{\odot}$ and temperatures below 1700–1600 K for subsolar metallicities and ages older than 1 Gyr, in the range for coolest L subdwarfs (e.g. 2MASS J05325346+8246465; Burgasser et al. 2008). However, because they are substellar, the atmospheres of these objects become exceedingly cold at the older ages expected for halo dwarfs. An object with [M/H] = −1.0 (−2.0) at the Li boundary mass has temperatures of <1000 K (1050 K) for ages larger than 5 Gyr, i.e. it is a T subdwarf. If Li chemistry follows solar metallicity trends, the atomic form will likely be depleted in such objects. On the other hand, it is possible that the Li condensation temperature is metallicity-dependent, just as mineral/metal condensate formation is inferred to be from observables (e.g. Burgasser et al. 2007) and models (e.g. Witte et al. 2009). The search for Li absorption in even cooler subdwarfs is thus critical for constraining metallicity dependencies on both the Li-burning and hydrogen-burning mass limits, and atmospheric chemistry.

[7] While ISM accretion is commonly modelled as Bondi-Hoyle accretion (e.g. Yoshii 1981; Frebel et al. 2009), the dynamics of a low-mass halo subdwarf moving through the ISM at high speed does not satisfy the conditions for this kind of accretion, as the dynamic scale, $GM/v^2 \approx 10^{10}$ cm, is much smaller than the ISM mean free path, $(\sigma_{\mathrm{ISM}} n_{\mathrm{ISM}})^{-1} \approx 3 \times 10^{15}$ cm, assuming $\sigma_{ISM} = \pi \times 10^{-16}$ cm^2 and $n_{\mathrm{ISM}} = 1$ cm^{-3} (Bondi & Hoyle 1944). Indeed, this condition is rarely satisfied for low-mass stars.

[8] The ISM is at rest relative to the local standard of rest, probably accurate to within +/−30 km s^{-1} (e.g. Frisch & Slavin 2006), so the relative speed is just the absolute value of $(U, V, W) = 325$ km s^{-1} which we rounded down.

8. Conclusions and outlook

We presented optical spectra of two mid-L subdwarfs and set upper limits on the pseudo-equivalent widths of the Li I doublet at 6707.8 Å. We can summarise our results as follows:

- We report the detection of a feature in the spectrum of SDSS1256 aligned with Li I at 6707.8 Å , but attributable to CaH. This sets a confusion limit for detectable Li abundance of [Li/H] = −3.
- We set an upper limit of 90 mÅ on the EW of the Li doublet for 2MASS1626, placing both objects in the Li-burning regime.
- We revise previous radial velocity measurements for both objects and derive new space motions and Galactic orbits, the latter confirming both sources as members of the inner halo population.
- We find that ISM accretion of Li-rich material would provide a basal abundance below our confusion limits, and constrain circumstellar accretion to be less than 10^9 g/yr on SDSS1256.
- We reproduced the observed spectrum of SDSS1256 based on NextGen atmosphere models with reduced metallicity and factors adjusting the amount of TiO and CaH molecules.

The next step is to attempt a detection in cooler L and T subdwarfs to reveal their true nature and place empirical constraint(s) on low-metallicity evolutionary models. Further photometric searches to uncover T subdwarfs will likely be needed in order to investigate the presence (or absence) of Li in metal-poor brown dwarfs. Moreover, additional work on the condensation of major chemistry features as a function of temperatures and pressures in metal-poor atmospheres is needed, similar to the work of Lodders (1999) for solar-type brown dwarfs.

Acknowledgements. N.L. was funded by the Ramón y Cajal fellowship number 08-303-01-02. This research has been supported by the Spanish Ministry of Economics and Competitiveness under the project AYA2010-19136. N.L. thanks Marcela Espinoza Contreras for her contribution during the submission of the proposals. The authors thank Isabelle Baraffe for her insight in the lithium boundary mass limits. A.J.B. was a visiting professor at the Instituto de Astrofísica de Canarias between September and December 2014 funded by the Tri-continental Talent programme (CEI Canarias: Campus Atlántico Tricontinental). This work is based on observations collected with FORS2 on the VLT at the European Southern Observatory, Chile, under programmes 089.C-0883 and 091.C-0594A. This work is also based on observations made with the Gran Telescopio Canarias (GTC), installed in the Spanish Observatorio del Roque de los Muchachos of the Instituto de Astrofísica de Canarias, in the island of La Palma (programmes GTC64_10B and GTC38_11A). This research has made use of the Simbad and Vizier databases, operated at the Centre de Données Astronomiques de Strasbourg (CDS), and of NASA's Astrophysics Data System Bibliographic Services (ADS).

References

Adelman-McCarthy, J. K., Agüeros, M. A., Allam, S. S., et al. 2007, ApJS, 172, 634
Adelman-McCarthy, J. K., et al. 2009, VizieR Online Data Catalog: II/294
Alexander, J. B. 1967, The Observatory, 87, 238
Allard, F., Hauschildt, P. H., Alexander, D. R., Tamanai, A., & Schweitzer, A. 2001, ApJ, 556, 357
Allard, F., Homeier, D., & Freytag, B. 2012, Roy. Soc. London Phil. Trans. Ser. A, 370, 2765
Appenzeller, I., Fricke, K., Fürtig, W., et al. 1998, The Messenger, 94, 1
Baraffe, I., Chabrier, G., Allard, F., & Hauschildt, P. H. 1997, A&A, 327, 1054
Baraffe, I., Chabrier, G., Allard, F., & Hauschildt, P. H. 1998, A&A, 337, 403
Baraffe, I., Chabrier, G., Barman, T. S., Allard, F., & Hauschildt, P. H. 2003, A&A, 402, 701
Basri, G., Marcy, G. W., & Graham, J. R. 1996, ApJ, 458, 600
Bildsten, L., Brown, E. F., Matzner, C. D., & Ushomirsky, G. 1997, ApJ, 482, 442
Bochanski, J. J., West, A. A., Hawley, S. L., & Covey, K. R. 2007, AJ, 133, 531
Bondi, H., & Hoyle, F. 1944, MNRAS, 104, 273
Bonifacio, P., Molaro, P., Sivarani, T., et al. 2007, A&A, 462, 851
Bovy, J., Allende Prieto, C., Beers, T. C., et al. 2012, ApJ, 759, 131
Burgasser, A. J. 2004, ApJ, 614, L73
Burgasser, A. J. 2007, ApJ, 658, 617
Burgasser, A. J., Kirkpatrick, J. D., Burrows, A., et al. 2003a, ApJ, 592, 1186
Burgasser, A. J., Kirkpatrick, J. D., Liebert, J., & Burrows, A. 2003b, ApJ, 594, 510
Burgasser, A. J., Cruz, K. L., & Kirkpatrick, J. D. 2007, ApJ, 657, 494
Burgasser, A. J., Vrba, F. J., Lépine, S., et al. 2008, ApJ, 672, 1159
Burgasser, A. J., Witte, S., Helling, C., et al. 2009, ApJ, 697, 148
Burke, C. J., Pinsonneault, M. H., & Sills, A. 2004, ApJ, 604, 272
Burrows, A., & Liebert, J. 1993, Rev. Mod. Phys., 65, 301
Burrows, A., & Sharp, C. M. 1999, ApJ, 512, 843
Burrows, A., Marley, M., Hubbard, W. B., et al. 1997, ApJ, 491, 856
Burrows, A., Hubbard, W. B., Lunine, J. I., & Liebert, J. 2001, Rev. Mod. Phys., 73, 719
Burrows, A., Ram, R. S., Bernath, P., Sharp, C. M., & Milsom, J. A. 2002, ApJ, 577, 986
Burrows, A., Sudarsky, D., & Lunine, J. I. 2003, ApJ, 596, 587
Carlberg, J. K., Smith, V. V., Cunha, K., Majewski, S. R., & Rood, R. T. 2010, ApJ, 723, L103
Carollo, D., Beers, T. C., Lee, Y. S., et al. 2007, Nature, 450, 1020
Cepa, J., Aguiar, M., Escalera, V. G., et al. 2000, in SPIE Conf. Ser. 4008, eds. M. Iye, & A. F. Moorwood, 623
Chabrier, G., & Baraffe, I. 1997, A&A, 327, 1039
Chabrier, G., & Baraffe, I. 2000, ARA&A, 38, 337
Cruz, K. L., Kirkpatrick, J. D., & Burgasser, A. J. 2009, AJ, 137, 3345
Cushing, M. C., Looper, D., Burgasser, A. J., et al. 2009, ApJ, 696, 986
Dulick, M., Bauschlicher, Jr., C. W., Burrows, A., et al. 2003, ApJ, 594, 651
Faherty, J. K., Beletsky, Y., Burgasser, A. J., et al. 2014, ApJ, 790, 90
Fields, B. D. 2011, Ann. Rev. Nucl. Part. Sci., 61, 47
Frebel, A., Johnson, J. L., & Bromm, V. 2009, MNRAS, 392, L50
Frisch, P. C., & Slavin, J. D. 2006, Astrophys. Space Sci. Trans., 2, 53
Gianninas, A., Bergeron, P., & Ruiz, M. T. 2011, ApJ, 743, 138
Gizis, J. E. 1997, AJ, 113, 806
Goldman, B., Bouy, H., Zapatero Osorio, M. R., et al. 2008, A&A, 490, 763
Gontcharov, G. A. 2006, Astron. Lett., 32, 759
Harrington, R. S., & Dahn, C. C. 1980, AJ, 85, 454
Hayashi, M., & Nakano, S. 1963, Progr. Theor. Phys., 30, 460
Høg, E., Fabricius, C., Makarov, V. V., et al. 2000, A&A, 355, L27
Israelian, G., Santos, N. C., Mayor, M., & Rebolo, R. 2001, Nature, 411, 163
Kalberla, P. M. W., & Kerp, J. 2009, ARA&A, 47, 27
King, R. R., McCaughrean, M. J., Homeier, D., et al. 2010, A&A, 510, A99
Kirkpatrick, J. D., Reid, I. N., Liebert, J., et al. 1999, ApJ, 519, 802
Kirkpatrick, J. D., Reid, I. N., Liebert, J., et al. 2000, AJ, 120, 447
Kirkpatrick, J. D., Cruz, K. L., Barman, T. S., et al. 2008, ApJ, 689, 1295
Kirkpatrick, J. D., Looper, D. L., Burgasser, A. J., et al. 2010, ApJS, 190, 100
Kirkpatrick, J. D., Schneider, A., Fajardo-Acosta, S., et al. 2014, ApJ, 783, 122
Kumar, S. S. 1963, ApJ, 137, 1126
Kupka, F., Piskunov, N., Ryabchikova, T. A., Stempels, H. C., & Weiss, W. W. 1999, A&AS, 138, 119
Leggett, S. K., Saumon, D., Marley, M. S., et al. 2012, ApJ, 748, 74
Lépine, S., & Shara, M. M. 2005, AJ, 129, 1483
Lodders, K. 1999, ApJ, 519, 793
Lodders, K. 2003, ApJ, 591, 1220
Lodders, K., & Fegley, Jr., B. 2006, Chemistry of Low Mass Substellar Objects, ed. J. W. Mason (Springer)
Lodieu, N., Zapatero Osorio, M. R., Martín, E. L., Solano, E., & Aberasturi, M. 2010, ApJ, 708, L107
Lodieu, N., Espinoza Contreras, M., Zapatero Osorio, M. R., et al. 2012, A&A, 542, A105
Lodieu, N., Zapatero Osorio, M. R., Rebolo, R., Béjar, V. J. S., & Pérez-Garrido, A. 2015, A&A, submitted
Magain, P. 1987, A&A, 179, 176
Magazzu, A., Martin, E. L., & Rebolo, R. 1991, A&A, 249, 149
Magazzu, A., Rebolo, R., & Pavlenko, I. V. 1992, ApJ, 392, 159
Mould, J. R., & Hyland, A. R. 1976, ApJ, 208, 399
Oppenheimer, B. R., Kulkarni, S. R., Matthews, K., & van Kerkwijk, M. H. 1998, ApJ, 502, 932
Pancino, E., Altavilla, G., Marinoni, S., et al. 2012, MNRAS, 426, 1767
Pavlenko, Y. V. 1998, Astron. Rep., 42, 787
Pavlenko, Y. V. 2014, Astron. Rep., 58, 825
Pavlenko, Y. V., Rebolo, R., Martín, E. L., & Garcia Lopez, R. J. 1995, A&A, 303, 807

Pavlenko, Y. V., Jones, H. R. A., Lyubchik, Y., Tennyson, J., & Pinfield, D. J. 2006, A&A, 447, 709
Pavlenko, Y. V., Jones, H. R. A., Martín, E. L., et al. 2007a, MNRAS, 380, 1285
Pavlenko, Y. V., Zhukovska, S. V., & Volobuev, M. 2007b, Astron. Rep., 51, 282
Plez, B. 1998, A&A, 337, 495
Rajpurohit, A. S., Reylé, C., Allard, F., et al. 2014, A&A, 564, A90
Rebolo, R., Beckman, J. E., & Molaro, P. 1988, A&A, 192, 192
Rebolo, R., Martín, E. L., & Magazzù, A. 1992, ApJ, 389, L83
Saumon, D., & Marley, M. S. 2008, ApJ, 689, 1327
Schilbach, E., Röser, S., & Scholz, R. 2009, A&A, 493, L27
Schönrich, R., Binney, J., & Dehnen, W. 2010, MNRAS, 403, 1829
Schultz, A. B., Allard, F., Clampin, M., et al. 1998, ApJ, 492, L181
Sion, E. M., Holberg, J. B., Oswalt, T. D., McCook, G. P., & Wasatonic, R. 2009, AJ, 138, 1681
Sivarani, T., Lépine, S., Kembhavi, A. K., & Gupchup, J. 2009, ApJ, 694, L140
Spergel, D. N., Bean, R., Doré, O., et al. 2007, ApJS, 170, 377
Spite, M., & Spite, F. 1982, Nature, 297, 483
Tinney, C. G. 1998, MNRAS, 296, L42
Tody, D. 1986, in SPIE Conf. Ser. 627, ed. D. L. Crawford, 733
Tody, D. 1993, in Astronomical Data Analysis Software and Systems II, eds. R. J. Hanisch, R. J. V. Brissenden, & J. Barnes, ASP Conf. Ser., 52, 173
van Altena, W. F., Lee, J. T., & Hoffleit, E. D. 1995, The general catalogue of trigonometric (stellar) parallaxes (New Haven: Yale University Observatory)
van Leeuwen, F. 2007, A&A, 474, 653
West, A. A., Hawley, S. L., Bochanski, J. J., et al. 2008, AJ, 135, 785
Witte, S., Helling, C., & Hauschildt, P. H. 2009, A&A, 506, 1367
Yoshii, Y. 1981, A&A, 97, 280
Zapatero Osorio, M. R., Béjar, V. J. S., Miles-Páez, P. A., et al. 2014, A&A, 568, A6